

1 New results in conventional and exotic spectroscopy

2 **Adriano Di Florio**^{a,*}

3 ^a*Università degli Studi di Bari Aldo Moro and I.N.F.N. - Sezione di Bari*

4 *E-mail: adriano.di.florio@cern.ch*

The present report summarises three recent CMS results in conventional and exotic spectroscopy. Firstly the search for a narrow resonance decaying to $Y(1S)\mu^+\mu^-$ performed with pp collision data collected in 2016 with the CMS detector at the LHC in proton-proton collisions at $\sqrt{s} = 13$ TeV, corresponding to an integrated luminosity of 35.9fb^{-1} . A tetraquark ($bb\bar{b}\bar{b}$) search is performed for masses in the vicinity of four times the bottom quark mass, between 17.5 and 19.5 GeV, while a generic search for other resonances is performed for masses between 16.5 and 27 GeV. No significant excess of events compatible with a narrow resonance is observed in the data. Limits on the production cross section times branching fraction of its decay to four muons via an intermediate $Y(1S)$ resonance are set as a function of the resonance mass.

In the second part, the study of $B^+ \rightarrow J/\psi\bar{\Lambda}p$, performed using pp collision data collected in 2012 at $\sqrt{s} = 8$ TeV, corresponding to an integrated luminosity of 19.6fb^{-1} , is presented. The ratio of branching fractions $\mathcal{B}(B^+ \rightarrow J/\psi\Lambda p)/\mathcal{B}(B^+ \rightarrow J/\psi K(892)^+)$ is measured to be $(1.054 \pm 0.057(\text{stat}) \pm 0.035(\text{syst}) \pm 0.011(\mathcal{B}))\%$. In addition the invariant mass distributions of the $J/\psi\Lambda$, $J/\psi p$, and Λp systems produced in the $B^+ \rightarrow J/\psi\bar{\Lambda}p$ decay are investigated. Using a model-independent angular amplitude analysis approach, it is shown that the observed invariant masses distributions are consistent with the contributions from excited kaons decaying to the Λp system.

Finally the study of excited Λ_b^0 baryons is reported, based on a data sample collected in 2016–2018 at a center-of-mass energy of 13 TeV, corresponding to an integrated luminosity of up to 140fb^{-1} . The existence of four excited Λ_b^0 states: $\Lambda_b(5912)^0$, $\Lambda_b(5920)^0$, $\Lambda_b(6146)^0$ and $\Lambda_b(6152)^0$ decaying to $\Lambda_b^0\pi^+\pi^-$ is confirmed. Also a broad excess of events in the $\Lambda_b^0\pi^+\pi^-$ mass distribution in the region of $6040 \div 6100$ MeV is observed.

BEAUTY2020

21-24 September 2020

Kashiwa, Japan (online)

*Speaker

1. Search for resonances decaying to $\Upsilon(1S)\mu^+\mu^-$

Quarkonium pair production is an important probe of both perturbative and nonperturbative processes in quantum chromodynamics. In [1] CMS measured the cross section for $\Upsilon(1S)$ pair production with both mesons decaying to $\mu\mu$ and it also performed a search for a narrow resonance decaying to $\Upsilon(1S)\mu^+\mu^-$. Such a resonance could indicate the existence of a tetraquark that is a bound state of two b quarks and two \bar{b} antiquarks. The search for $bb\bar{b}\bar{b}$ tetraquarks is performed for $17.5 \leq m(4\mu) \leq 19.5$ GeV, while the generic search for a narrow resonance is done for $16.5 \leq m(4\mu) \leq 27$ GeV. In both cases the $\Upsilon(1S)$ pair production serves as a reference, since the final state is the same and a similar event selection is used. The measurement of the $\Upsilon(1S)$ pair production cross section is reported in another conference contribution. The paper relies on proton-proton collision data collected at $\sqrt{s} = 13$ TeV by the CMS detector in 2016 ($\mathcal{L}_{int} = 35.9\text{fb}^{-1}$).

Events are selected with a trigger that requires the presence of three muons, among which two must have an invariant mass compatible with a Υ resonance ($8.5 < m(\mu\mu) < 11.4$ GeV) and the dimuon vertex fit probability must be greater than 0.5%. Each event is then required to have four reconstructed muons with $p_T(\mu) > 2\text{GeV}$ and $|\eta(\mu)| < 2.4$. For each event, the combination of four muons with the largest χ^2 probability is chosen and a $p_T(\mu)2.5$ GeV cut is applied. The event is discarded if one of the two alternative opposite sign muon pairs has an invariant mass either compatible with a $J\psi$ particle or lower than 4 GeV.

For the resonance search, $m(\Upsilon(1S))$ is also required to be within 2σ of the experimental resolution (between 0.06 and 0.15 GeV) from the $\Upsilon(1S)$ nominal mass [2]. Assuming that the resonant state decays into two muons and a $\Upsilon(1S)(\rightarrow \mu\mu)$, the signal mass resolution is improved by using the observable [3]: $\tilde{m}_{4\mu} = m_{4\mu}m_{\mu\mu} + m_{\Upsilon(1S)}$; where $m_{4\mu}$ is the invariant mass of the four leptons, $m_{\mu\mu}$ the invariant mass associated with the $\Upsilon(1S)$ candidate, and $m_{\Upsilon(1S)}$ the nominal mass of the $\Upsilon(1S)$ particle (9.46 GeV [2]). This $\tilde{m}_{4\mu}$ has a resolution about 50% better than $m_{4\mu}$ for signal events.

Multiple models are taken into account for the narrow resonance: a bottomonium state with the properties of the $\chi_{b1}(1P)$, assuming a phase-space decay to a $\Upsilon(1S)$ meson and a pair of muons (simulated with *PYTHIA* 8.226 generator [6]); a scalar, pseudoscalar and a spin-2 particle produced in gluon fusion (simulated with *JHUGEN* generator [7]). For each model, four resonance mass values are simulated: 14, 18, 22, and 26 GeV. The signal distributions are parameterised by the sum of two Gaussian functions with the same mean and parameters that are determined from the simulated signal samples.

One of the background components comes from the $\Upsilon(1S)\Upsilon(1S)$ process. It is modelled as the product of a sigmoid function and an exponential function with a negative exponent. The nominal model for the invariant mass of this background is taken as an average between the DPS (double parton scattering) and SPS (single parton scattering) templates, with the DPS fraction estimated, in the same paper, from the pair production cross section measurement ($f_{DPS} = 0.39 \pm 0.14$). The number of $\Upsilon(1S)\Upsilon(1S)$ events in the signal region is extracted from a 2D fit to the invariant masses of the two muon pair without applying the acceptance and efficiency corrections. Only events with $13 < \tilde{m}_{4\mu} < 28$ GeV are retained and no rapidity criteria are applied for the reconstructed $\Upsilon(1S)$ candidates. The yield is measured to be 78 ± 13 events. The requirement that the mass of a dimuon pair is compatible with the mass of a $\Upsilon(1S)$ meson within 2σ is not applied to extract

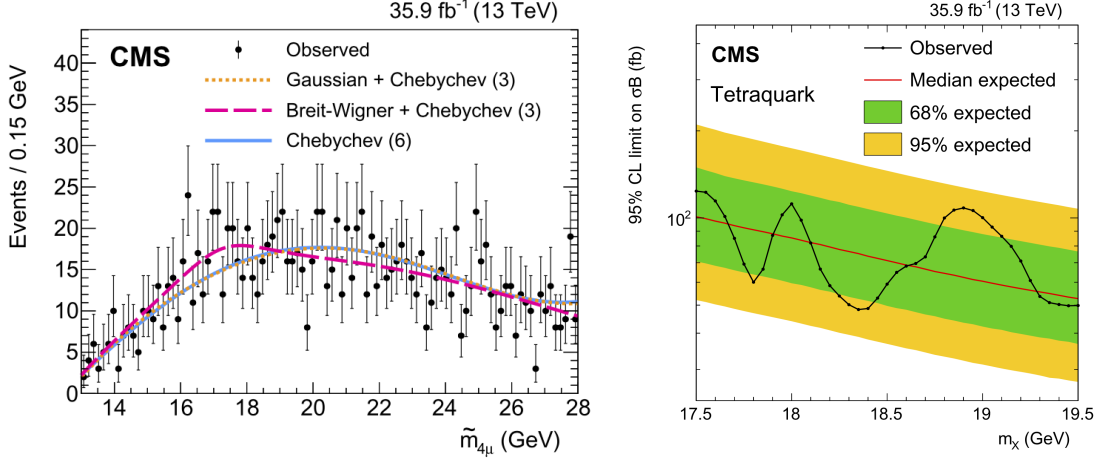


Figure 1: Left: The $\tilde{m}_{4\mu}$ distribution from data and the results of the fit in the resonance search. An example signal, with 1σ significance, is shown for the tetraquark model with a mass of 19 GeV. Right: Upper limits at 95% CL on the product of the cross section and branching fraction for a tetraquark, where σ denotes the production cross section of the resonance, and $\mathcal{B} = \mathcal{B}(X \rightarrow \Upsilon(1S)\mu\mu) \cdot \mathcal{B}(\Upsilon(1S) \rightarrow \mu\mu)$.

48 the yield because the 2D fit relies on the mass tails to estimate the combinatorial background.
 49 Since the efficiency of this criterion is 95% in both the SPS and DPS $\Upsilon(1S)\Upsilon(1S)$ simulations, the
 50 $\Upsilon(1S)\Upsilon(1S)$ yield in the signal region is corrected to 74 ± 13 .

51 The combinatorial background in the $\tilde{m}_{4\mu}$ spectrum is obtained by fitting the data in the signal
 52 region. Several generic functions are used to parameterise this smooth background: Chebychev
 53 polynomials of various orders, the sum of a Gaussian and a Chebychev polynomial, the sum of a
 54 Breit–Wigner and a Chebychev polynomial. The compatibility of such forms with the smooth $\tilde{m}_{4\mu}$
 55 spectrum of the combinatorial background is checked and confirmed using a control region where
 56 the vertex fit χ^2 probability of the four muons is in the range of $10^{-10} - 10^{-3}$. The parameters of
 57 the functions, as well as the choice of the functional form, are freely floating in the fit to the signal
 58 region. Multiple sources of systematic uncertainty are taken into account, such as, citing the most
 59 important: the integrate luminosity estimation, the trigger and the muon identification efficiencies,
 60 the signal and background modelling and the limited size of the simulated samples.

61 The $\tilde{m}_{4\mu}$ distribution in the signal region of the resonance search is shown in the left panel
 62 of Fig. 1. The background and example signal components are shown using their best-fit shapes
 63 and normalisations. No significant narrow excess of events is observed above the background
 64 expectation.

65 Upper limits on the product of the production cross section of a resonance and the branching
 66 fraction to a final state of four muons via an intermediate $\Upsilon(1S)$ resonance are set at 95% confidence
 67 level (CL) using the modified frequentist construction CLs in the asymptotic approximation [4][5],
 68 separately for each signal model. Masses between 17.5 and 19.5 GeV are probed in the context
 69 of the tetraquark search (see Figure 1), using the bottomonium model, whereas the limits in the
 70 extended mass range $16.5 \div 27$ GeV are set for the generic search. The largest excess is observed for
 71 a resonance mass of 25.1 GeV, and has a local significance of 2.4σ for the scalar signal hypothesis.
 72 In conclusion, no excess of events compatible with a signal is observed in the four-muon invariant
 73 mass spectrum and this statement would need to be reassessed with the full Run2 statistics.

74 2. Study of the $B^+ \rightarrow J/\psi \bar{\Lambda} p$ decay

75 The $B^+ \rightarrow J/\psi \bar{\Lambda} p$ decay is the first observed example of a B meson decay into baryons and a
 76 charmonium state. In [8] a study is reported of the $B^+ \rightarrow J/\psi \bar{\Lambda} p$ ($J/\psi \rightarrow \mu^+ \mu^-$, $\bar{\Lambda} \rightarrow p \pi^+$) decay
 77 using a data sample of pp collisions collected by the CMS experiment in 2012 at $\sqrt{s} = 8$ TeV
 78 ($\mathcal{L}_{int} = 19.6 \text{ fb}^{-1}$). The decay $B^+ \rightarrow J/\psi K^{*+}$ ($K^{*+} \rightarrow K_S^0 \pi^+ \rightarrow \pi^+ \pi^- \pi^+$) is chosen as the
 79 normalisation channel (where K^{*+} denotes the $K^*(892)^+$ particle). The ratio of the branching
 80 fractions is measured as: $\frac{\mathcal{B}(B^+ \rightarrow J/\psi \bar{\Lambda} p)}{\mathcal{B}(B^+ \rightarrow J/\psi K^{*+})} = \frac{N(B^+ \rightarrow J/\psi \bar{\Lambda} p) \mathcal{B}(K^{*+} \rightarrow K_S^0 \pi^+) \mathcal{B}(K_S^0 \rightarrow \pi^+ \pi^-) \epsilon(B^+ \rightarrow J/\psi K^{*+})}{N(B^+ \rightarrow J/\psi K^{*+}) \mathcal{B}(\bar{\Lambda} \rightarrow p \pi^+) \epsilon(B^+ \rightarrow J/\psi \bar{\Lambda} p)}$;
 81 where N and ϵ correspond to the total yield and the total efficiency of the decay, respectively.
 82 Data were collected with a dedicated trigger, optimised for the selection of b hadrons decaying
 83 to $J/\psi (\rightarrow \mu^+ \mu^-)$. The final B^+ candidate is built combining the J/ψ candidate with a positively
 84 charged particle track, assumed to be a p track, and a $\bar{\Lambda}$ candidate, formed from displaced two prong
 85 vertices under the assumption of the $\bar{\Lambda} \rightarrow p \pi^+$ decay [9]. A further selection on the displacement
 86 and the pointing angle is applied, in order to remove most of the combinatorial background.
 87 Contamination from $K_S^0 \rightarrow \pi^- \pi^+$ decays is removed.

88 The normalisation decay channel $B^+ \rightarrow J/\psi K^{*+}$ candidates are built using the same recon-
 89 struction chain. The distribution of $M(B^+ \rightarrow J/\psi \bar{\Lambda} p)$ is shown in Figure 2 resulting in a signal
 90 yield of 452 ± 23 events. To extract the K^{*+} meson contribution, *sPlot* technique [10] is used with
 91 $M(J/\psi K_S^0 \pi^+)$ as discriminating variable. The $B^+ \rightarrow J/\psi K^{*+}$ signal yield (20863 ± 357) is then
 92 extracted integrating the signal fit over ± 50 MeV around the K^{*+} mass.

93 The efficiency for detecting and identifying the B^+ decays is calculated using simulated signal
 94 samples. The efficiency ratio is found to be $\epsilon(B^+ \rightarrow J/\psi K^{*+})/\epsilon(B^+ \rightarrow J/\psi \bar{\Lambda} p) = 1.347 \pm$
 95 $0.023(\text{stat})$. Multiple systematic uncertainty sources are taken into account, due to the choice of the
 96 background and signal models, to the discrepancy between data and simulation and the limited size
 97 of the simulated samples. Using the world-average values of the $\mathcal{B}(K^{*+} \rightarrow K_S^0 \pi^+)$, $\mathcal{B}(K_S^0 \rightarrow \pi^+ \pi^-)$,
 98 $\mathcal{B}(\bar{\Lambda} \rightarrow p \pi^+)$ branching fractions [2], the ratio $\mathcal{B}(B^+ \rightarrow J/\psi \bar{\Lambda} p)/\mathcal{B}(B^+ \rightarrow J/\psi K^{*+})$ is found to
 99 be $(1.054 \pm 0.057(\text{stat}) \pm 0.035(\text{syst}) \pm 0.011(\mathcal{B}))\%$, where the third uncertainty comes from the
 100 world-average branching fractions of the decays involved. From this ratio and the world-average
 101 value of $\mathcal{B}(B^+ \rightarrow J/\psi K^{*+}) = (1.43 \pm 0.08) \times 10^{-3}$ [2], the branching fraction $\mathcal{B}(B^+ \rightarrow J/\psi \bar{\Lambda} p) =$
 102 $(15.1 \pm 0.8(\text{stat}) \pm 0.5(\text{syst}) \pm 0.9(\mathcal{B})) \times 10^{-6}$ is also obtained. Furthermore the invariant mass
 103 distributions of the $J/\psi \bar{\Lambda}$, $J/\psi p$ and $\bar{\Lambda} p$ two-body combinations of the $B^+ \rightarrow J/\psi \bar{\Lambda} p$ decay
 104 products have been investigated. Figure 2 shows the efficiency-corrected and *sPlot* background-
 105 subtracted ($M(J/\psi \bar{\Lambda} p)$ being the discriminating variable) distributions of $M(J/\psi p)$, $M(J/\psi \bar{\Lambda})$,
 106 and $M(\bar{\Lambda} p)$. None of them can be adequately described by a pure three-body non-resonant phase
 107 space decay hypothesis (H_{PS}). There are, in fact, at least three known K^{*+} resonances that can
 108 decay to $\bar{\Lambda} p$ and may contribute to the $M(J/\psi p)$ and $M(J/\psi \bar{\Lambda})$ distributions. To account for these
 109 possible contributions, a model independent approach developed by BaBar[11] was used. It takes
 110 into account the K^{*+} introducing an angular structure into the simulated samples by applying the
 111 appropriate weights, originating from the $\cos(\theta_{K^*})$ expansion in terms of Legendre polynomials:
 112 where $\langle P_j^N \rangle = 2 \langle P_j^U \rangle / N_{reco}^{corr}$ are the normalised Legendre moments [8]; N_{reco}^{corr} is the
 113 corrected number of reconstructed events in each $M(\bar{\Lambda} p)$ bin; $l_{max} = 8$, i.e. twice the maximum
 114 spin of the considered K^{*+} resonances.

115 In addition the simulation is also weighted to reproduce the $M(\bar{\Lambda} p)$ spectrum observed in data,

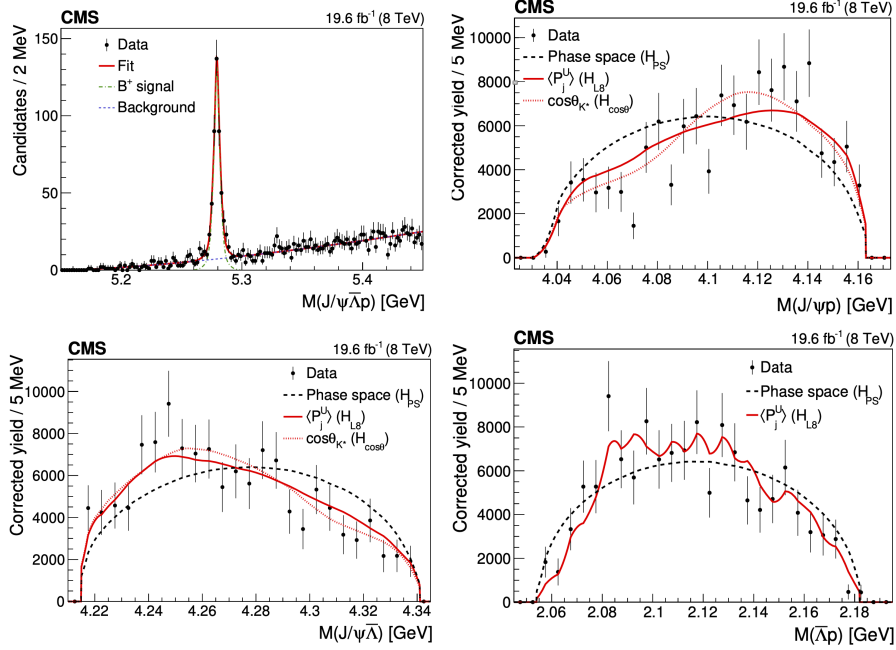


Figure 2: The invariant mass distribution of the selected $B^+ \rightarrow J/\psi \bar{\Lambda} p$ candidates (upper left). The invariant mass distributions of the $J/\psi p$ (upper right), $J/\psi \bar{\Lambda}$ (bottom left), and $J/\psi p$ (bottom right) systems from the $B^+ \rightarrow J/\psi p$ decay. The points show the efficiency-corrected, background-subtracted data. Superimposed curves are obtained from simulation for the different hypotheses described in the text: H_{PS} (dashed lines), H_{L8} (solid curves), $H_{\cos(\theta)}$ (dotted curves).

116 using a linear interpolation of the data-to-simulation ratio histogram. Results of both procedures
 117 are shown in Figure 2 (solid line) and it is clear that the description of the three mass is quite
 118 improved. The compatibility of the data with both H_{PS} and phase space augmented with the
 119 reweighing hypothesis (H_{L8}) is quantified using the likelihood ratio technique, using as null-
 120 hypothesis an additional hypothesis $H_{\cos(\theta)}$ that accounts for all the features in the $\cos(\theta_{K^*})$ and
 121 $M(\bar{\Lambda} p)$ distributions observed in data.

122 Multiple systematic uncertainty contributions are taken into account, due to the choice of
 123 the background p.d.f. used in the $M(J/\psi \bar{\Lambda} p)$ fit; to the selection of the $B^+ \rightarrow J/\psi \bar{\Lambda} p$;
 124 to the statistical fluctuations in the 2D efficiency calculation. The effect of the correlation between
 125 $M(\bar{\Lambda} p)$, $\cos(\theta_{K^*})$, $M(J/\psi p)$, and $M(J/\psi \bar{\Lambda})$ is also taken into account. The significance of the
 126 incompatibility of data with the H_{PS} hypothesis is then found to vary from 6.1 to 8.1, 5.5 to
 127 7.4, and 3.4 to 4.8 standard deviations for the $J/\psi p$, $J/\psi \bar{\Lambda}$, and $\bar{\Lambda} p$ invariant mass distributions,
 128 respectively. The incompatibility of data with H_{L8} varies from 1.3 to 2.8 (2.7) standard deviations
 129 for the $J/\psi p$ ($J/\psi \bar{\Lambda}$) invariant mass spectrum. This allows us to conclude that the data are consistent
 130 with the H_{L8} hypothesis.

131 3. Study of excited Λ_b^0 states decaying to $\Lambda_b^0 \pi^+ \pi^-$

132 Spectroscopy of baryons that contain a heavy-flavor quark, such as the Λ_b^0 baryon, is a very
 133 important probe to test predictions of heavy-quark effective theory [12]. In [13] the CMS Collabo-
 134 ration reported a study of the $\Lambda_b^0 \pi^+ \pi^-$ invariant mass distribution in the 5900 ÷ 6400 MeV range.

135 The ground state baryon Λ_b^0 is reconstructed via its decays into the $J/\psi\Lambda$ and $\psi(2S)\Lambda$ channels. The
 136 analysis uses the pp collision data recorded with the CMS detector in 2016–2018 at $\sqrt{s} = 13$ TeV
 137 ($\mathcal{L}_{int} = 140 \text{ fb}^{-1}$).

138 The event selection begins by building a dimuon system with two opposite sign (OS) muons
 139 with $2.90 < M(\mu\mu) < 3.95 \text{ GeV}$ and which is taken to be a J/ψ candidate if $M(\mu\mu) < 3.4 \text{ GeV}$
 140 or a $\psi(2S)$ candidate otherwise. Also the $\psi(2S) \rightarrow J/\psi\pi\pi \rightarrow \mu\mu\pi\pi$ channel is considered. A Λ
 141 candidate is formed from a displaced two-prong vertex, assuming the decay $\Lambda \rightarrow p\pi$ [9]. To form
 142 the Λ_b^0 candidates, the J/ψ or $\psi(2S)$ candidate and the Λ candidate are fit to a common vertex, with
 143 J/ψ or $\psi(2S)$ mass constraint applied. A further selection on vertex association, displacement and
 144 pointing angle is carried on and several simulated signal samples with different masses of excited
 145 Λ_b^0 states are used in the analysis to optimise the selection criteria. The $\Lambda_b^0\pi^+\pi^-$ candidates are
 146 formed by combining the selected Λ_b^0 candidates with two OS tracks originating from the primary
 147 vertex. Combinations with two prompt same-sign (SS) pions are used as a control channel. To
 148 improve the $\Lambda_b^0\pi^+\pi^-$ invariant mass resolution by up to 50%, all tracks forming the PV and the
 149 selected Λ_b^0 candidate, taken as a single “pseudo-track”, are refit to a common vertex. The observed
 150 invariant mass distribution $m_{\Lambda_b^0\pi^+\pi^-}$ of the selected signal candidates near the threshold is shown
 151 in Figure 3. The best-fit signal yields are 28.4 ± 5.8 and 159 ± 14 events, the measured masses
 152 are $5912.32 \pm 0.12(\text{stat}) \text{ MeV}$ and $5920.16 \pm 0.07(\text{stat}) \text{ MeV}$ and the statistical significance of the
 153 peaks are $5.4 \div 5.7\sigma$ and well over 6σ , for the $\Lambda_b(5912)^0$ and $\Lambda_b(5920)^0$ states, respectively.

154 Higher masses in the $m_{\Lambda_b^0\pi^+\pi^-}$ distribution are studied as well, as shown in Figure 3. A narrow
 155 $\Lambda_b^0\pi^+\pi^-$ peak at approximately 6150 MeV is evident, consistent with an overlap of the $\Lambda_b(6146)^0$
 156 and $\Lambda_b(6152)^0$ signals, as well as a broad enhancement in the region below 6100 MeV. None of
 157 these features are present in the SS control region. A number of cross-checks have been performed
 158 to asses that the broad enhancement is not the result of a partially reconstructed decay, such as
 159 $\Lambda_b(6146)^0$ or $\Lambda_b(6152)^0$ decay into $\Lambda_b^0\pi^+\pi^-\pi^0$ (with a lost π^0); or a kinematic reflection, such as
 160 some state decaying into $\Lambda_b^0 K^\pm\pi^\mp$. In addition the 2D distributions of the $\Lambda_b^0\pi^+\pi^-$ mass versus the
 161 $\Lambda_b^0\pi^-$ and $\Lambda_b^0\pi^+$ masses were inspected. If the $\Lambda_b^0\pi^\pm$ invariant mass ranges corresponding to the
 162 Σ_b^+ , Σ_b^- , Σ_b^{*-} and Σ_b^{*+} baryons are vetoed, both the SS and OS mass distributions do not exhibit any
 163 broad enhancement. This suggests that the broad excess might be related to the intermediate Σ_b^\pm
 164 and Σ_b^\pm baryon states, although the current size of the data set does not allow this hypothesis to be
 165 properly tested.

166 The fit results for the yields and masses, respectively, are 301 ± 72 and $6073 \pm 5 \text{ MeV}$ for the broad
 167 enhancement, 70 ± 35 and $6146.5 \pm 1.9 \text{ MeV}$ for the $\Lambda_b(6146)^0$, and 113 ± 35 and $6152.7 \pm 1.1 \text{ MeV}$
 168 for the $\Lambda_b(6152)^0$. The measured natural width of the broad excess is $55 \pm 11(\text{stat}) \text{ MeV}$.

169 Several sources of systematic uncertainties in the measured masses are considered such as
 170 the choice of the fit model, the inclusion of the broad excess in the fit, the mass range for the fit,
 171 the peaks mass resolutions, determined from simulated samples; and the knowledge of the signal
 172 natural widths, taken from the ones measured by LHCb [14].

173 Using the likelihood-ratio technique the one-peak versus two-peak hypotheses for the 6150
 174 MeV structure have been tested and the presence of two peaks has a statistical significance of 0.4σ .
 175 The local statistical significance of the single-peak hypothesis with respect to the background-only
 176 hypothesis is found to be between 5.4σ and 6.5σ (changes due to the systematic uncertainties).

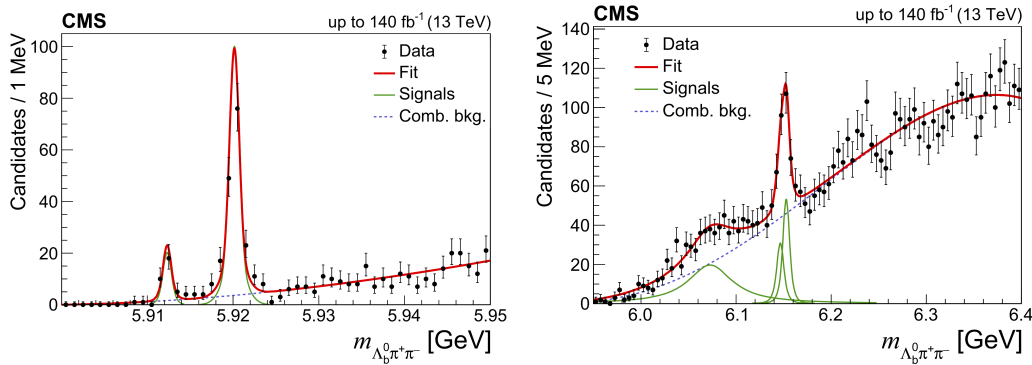


Figure 3: Invariant mass distribution of the selected $\Lambda_b^0 \pi^+ \pi^-$ candidates near threshold (left) and in the high-mass region (right). The overall fit result is shown by the thick solid line, with the thin and dashed lines representing the signal and combinatorial background components, respectively.

177 The broad enhancement has a local statistical significance of about 4σ . Resonances with masses
 178 between 6200 and 6400 MeV have been also considered in the fit model and no significant excess was
 179 found. In summary the measured masses are: $M(\Lambda_b(5912)^0) = 5912.32 \pm 0.12 \pm 0.01 \pm 0.17$ MeV,
 180 $M(\Lambda_b(5920)^0) = 5920.16 \pm 0.07 \pm 0.01 \pm 0.17$ MeV, $M(\Lambda_b(6146)^0) = 6146.5 \pm 1.9 \pm 0.8 \pm 0.2$ MeV,
 181 $M(\Lambda_b(6152)^0) = 6152.7 \pm 1.1 \pm 0.4 \pm 0.2$ MeV, where the first uncertainty is statistical, the second
 182 is systematic and the third is the uncertainty in the world-average Λ_b^0 mass [2].

183 References

- 184 [1] CMS Collaboration, *Measurement of the $\Upsilon(1S)$ pair production cross section and search for*
 185 *resonances decaying to $\Upsilon(1S)\mu^+\mu^-$ in proton-proton collisions at $\sqrt{s} = 13$ TeV*, *Phys. Lett. B*
 186 **808** (2020), 135578
- 187 [2] Particle Data Group, *Review of Particle Physics*, *Phys. Rev. D* **98** (2018) no.3, 030001
- 188 [3] CMS Collaboration, *Search for Higgs boson pair production in the $\gamma\gamma b\bar{b}$ final state in pp*
 189 *collisions at $\sqrt{s} = 13$ TeV*, *Phys. Lett. B* **788** (2019), 7-36
- 190 [4] ATLAS, CMS and LHC Higgs Combination Group, *Procedure for the LHC Higgs boson*
 191 *search combination in summer 2011*, ATL-PHYS-PUB-2011-011.
- 192 [5] G. Cowan, K. Cranmer, E. Gross and O. Vitells, *Asymptotic formulae for likelihood-based*
 193 *tests of new physics*, *Eur. Phys. J. C* **71** (2011), 1554
- 194 [6] T. Sjöstrand, S. Ask, J. R. Christiansen, R. Corke, N. Desai, P. Ilten, S. Mrenna, S. Pres-
 195 *tel*, C. O. Rasmussen and P. Z. Skands, *Comput. Phys. Commun.* **191** (2015), 159-177
 196 doi:10.1016/j.cpc.2015.01.024 [arXiv:1410.3012 [hep-ph]].
- 197 [7] Jeffrey Davis, Jeffrey (Heshy) Roskes, Ulascan Sarica, Markus Schulze <https://spin.pha.jhu.edu>
 198 .
- 199 [8] A. M. Sirunyan *et al.* [CMS], *Study of the $B^+ \rightarrow J/\psi \bar{\Lambda} p$ decay in proton-proton collisions at*
 200 $\sqrt{s} = 8$ TeV, *JHEP* **12** (2019), 100

- 201 [9] CMS Collaboration, *CMS Tracking Performance Results from Early LHC Operation*, *Eur.*
202 *Phys. J. C* **70** (2010), 1165-1192
- 203 [10] M. Pivk and F. R. Le Diberder, *SPlot: A Statistical tool to unfold data distributions*, *Nucl.*
204 *Instrum. Meth. A* **555** (2005), 356-369
- 205 [11] B. Aubert *et al.* [BaBar], *Search for the Z(4430)- at BABAR*, *Phys. Rev. D* **79** (2009), 112001
- 206 [12] Y. Chen, A. Fujimori, T. Müller, W. Stwalley, J. Yang (Eds.), *Heavy Quark Effective Theory*,
207 Springer, Berlin, Heidelberg, 2004.
- 208 [13] CMS Collaboration, *Study of excited Λ_b^0 states decaying to $\Lambda_b^0 \pi^+ \pi^-$ in proton-proton collisions*
209 *at $\sqrt{s} = 13$ TeV*, *Phys. Lett. B* **803** (2020), 135345
- 210 [14] LHCb Collaboration, *Observation of excited Λ_b^0 baryons*, *Phys. Rev. Lett.* **109** (2012), 172003